Correlation between the electronic structures and diffusion paths of interstitial defects in semiconductors: The case of CdTe

Jie Ma, Jihui Yang, and Su-Huai Wei*
National Renewable Energy Laboratory, Golden, Colorado 80401, USA

Juarez L. F. Da Silva
São Carlos Institute of Chemistry, University of São Paulo, São Carlos, São Paulo, Brazil

(Received 9 July 2014; revised manuscript received 2 September 2014; published 30 October 2014)

Using first-principles calculations, we study the diffusions of interstitial defects Cd, Cu, Te, and Cl in CdTe. We find that the diffusion behavior is strongly correlated with the electronic structure of the interstitial diffuser. For Cd and Cu, because the defect state is the nondegenerated s-like state under the T_d symmetry, the diffusions are almost along the ⟨111⟩ directions between the tetrahedral sites, although the diffusion of Cu shows some deviation due to the coupling between the Cu d and host s orbitals. The diffusions of the neutral and charged Cd and Cu follow similar paths. However, for Te and Cl atoms, because the defect state is the degenerated p-like state under the T_d symmetry, large distortions occur. Therefore the diffusion paths are very different from those of the interstitial Cd and Cu atoms, and depend strongly on the charge states of the interstitial atoms. For Te, we find that the distortion is mostly stabilized by the crystal-field splitting, but for Cl, the exchange splitting plays a more important role.

DOI: 10.1103/PhysRevB.90.155208 PACS number(s): 66.30.Dn, 61.72.jj, 61.72.uj, 71.55.Gs

I. INTRODUCTION

Atomic diffusion in semiconductor compounds plays an important role in determining their material properties, such as the doping limit, passivation, and stability of devices [1–5]. For example, CdTe is one of the most promising candidates for thin-film photovoltaic applications, because it has a nearly ideal direct band gap of ∼1.5 eV with a high absorption coefficient [6,7] and it is easy to grow. So far, CdTe solar cell efficiency above 20.4% [8] has been achieved. Experimentally, it has been well known that the postgrowth Cl and Cu treatments are very important for CdTe solar cells [9]. Without these treatments, CdTe is almost intrinsic (the hole concentration is very low, $<10^{14}$ cm^{-3}) with short minority carrier lifetime (<1 ns), and the efficiency is low (<10%) [9,10]. Theoretically, it has been found that both Cl and Cu can help to passivate the dangling-bond states at grain boundaries in CdTe, and the incorporation of proper amounts of Cu and Cl can also enhance the p-type doping by forming Cu on Cd site (Cu_{Cd}) and the A-center ($V_{Cd} + Cl_{Te}$) acceptors [11,12]. It has been well known that the diffusion behavior of interstitial elements in semiconductors is greatly influenced by its electronic structures [13,14]. However, it is not clear how Cu and Cl atoms diffuse from the back contact into the CdTe layer. Furthermore, when impurities such as Cu and Cl diffuse into the host, host elements such as Cd or Te atoms are often kicked out from the lattice sites and will diffuse away. Thus the diffusions of Cd and Te atoms are also important issues. However, the interstitial diffusions of Cd and Te also have not been systematically discussed.

CdTe is a zinc-blende-structure material with the T_d crystal symmetry. At T_d symmetry sites, the sp^3 orbitals are splitted into a singlet a_1 state and triplet t_2 states. The electrons of the interstitial atoms will fill into these a_1 and t_2 states. For cation atoms (Cd and Cu), the number of the valence electrons is equal to or less than two (d electrons are not counted), so the defect state is the singlet a_1 state. For anion atoms (Te and Cl), on the other hand, because the number of the valence electrons is greater than two but less than eight, after filling the energetically low-lying a_1 state [generally speaking, the energy of the fully occupied a_1 state is far below that of the valence-band maximum (VBM)], the defect electrons partially occupy the degenerated t_2 states. Electronically, if the degenerated levels are not fully occupied, the system may undergo some distortion that splits the degenerated levels. In this case, the system gains electronic energy from the level splitting but pays strain energy. Therefore the anion atoms (Te and Cl) may have very different diffusion behaviors compared to the cation atoms (Cd and Cu). However, how exactly the electronic structure affects the diffusion behavior is still not clear yet.

In this paper, using first-principles calculations, we have studied the diffusion behaviors of the cation atoms (Cd and Cu) and the anion atoms (Te and Cl) at both neutral and charged states. We find that the diffusions of the two cation atoms are almost along the ⟨111⟩ directions between the tetrahedral sites, although the diffusion of Cu slightly deviates from the exact ⟨111⟩ directions due to the coupling between the Cu d and host s orbitals. The diffusions of the neutral and charged cation atoms follow similar paths. However, the diffusions of the anion atoms are very different, due to the structural distortions. The anion diffusions are not along the ⟨111⟩ directions, and the neutral atoms diffuse differently from the charged atoms, due to different level splittings. For Te atom, we find that the structural distortion is benefited from the crystal-field splitting, and for Cl atom, the exchange splitting plays a more important role.

II. THEORETICAL APPROACH AND COMPUTATIONAL DETAILS

Our calculations were based on spin-polarized density functional theory (DFT) [15] within the generalized

*Corresponding author: suhuai.wei@nrel.gov

gradient approximation (GGA) formulated by Perdew, Burke, and Ernzerhof (PBE) [16] as implemented in the Vienna *ab initio* simulation package (VASP) [17]. The valence electrons (Cu $3d^{10}4s^1$, Cl $3s^23p^5$, Cd $4d^{10}5s^2$, and Te $5s^25p^4$) were described by the projected augmented wave (PAW) method [18] and the valence wave functions were expanded in a plane-wave basis with an energy cutoff of 300 eV. To study the diffusions in CdTe, we employed a 64-atom cubic supercell. The $2 \times 2 \times 2$ k-point mesh was employed for the Brillouin zone (BZ) integration. To obtain the diffusion paths and diffusion barrier energies, we employed the nudged elastic band (NEB) method [19] as implemented in VASP.

III. RESULTS AND DISCUSSION

A. Cation diffusions

In this section, we will discuss the diffusions of two cation atoms, namely, Cd and Cu. We find that because the defect electrons occupy only the nondegenerated a_1 state, there are only small structural distortions, depending on the strength of the coupling between the diffuser d and host s orbitals. Therefore the diffusions are almost along ⟨111⟩ directions between the tetrahedral sites.

1. Cd *diffusion*

The interstitial Cd is a deep double donor [14,20], and it can exist in three possible charge states: neutral, 1+, and 2+ charged states, depending on the relative position of the Fermi energy. The most stable interstitial site for the neutral Cd is the tetrahedral site surrounded by host cation (Cd) atoms, which is labeled as T_c here. It can be explained as follows: the T_c site has less electrons than the tetrahedral T_a site that is surrounded by host anion (Te) atoms, and hence, it has more space to accommodate the interstitial atom. For the charged Cd (Cd^+ and Cd^{2+}), the most stable site is the T_a site due to the reduced size of the positively charged interstitial ion and the increased Coulomb binding between the positively charged interstitial ion and the neighboring negatively charged Te ions. Our calculated total energy differences between the two tetrahedral sites, $E_{\rm tot}(T_c) - E_{\rm tot}(T_a)$, increase from −0.2 to 0.02 to 0.4 eV as the interstitial Cd atom becomes more positively charged.

The diffusion path of the interstitial Cd is displayed in Fig. 1(a). The diffusion paths of the neutral, 1+, and 2+ charged Cd atoms are almost the same. Basically, the interstitial Cd first diffuses along the [111] direction from the T_c site to a nearby T_a site, and then diffuses along the $[11\bar{1}]$ direction from the T_a site to another T_c site. Eventually, Cd diffuses from the T_c site to another nearby T_c site along the [110] direction. The diffusion energy curves of the interstitial Cd at all charge states are displayed in Fig. 1(b). For neutral Cd, the diffusion barrier site appears in between the two tetrahedral sites, which is labeled as M here, with an energy barrier of ∼0.52 eV. The Coulomb interaction between the neutral diffuser and the host is weak, so the strain effect is dominant. As Cd moves away from the tetrahedral site, there is less space around it and thus the strain energy increases. The M site has the least space along the ⟨111⟩ directions, so it has the highest

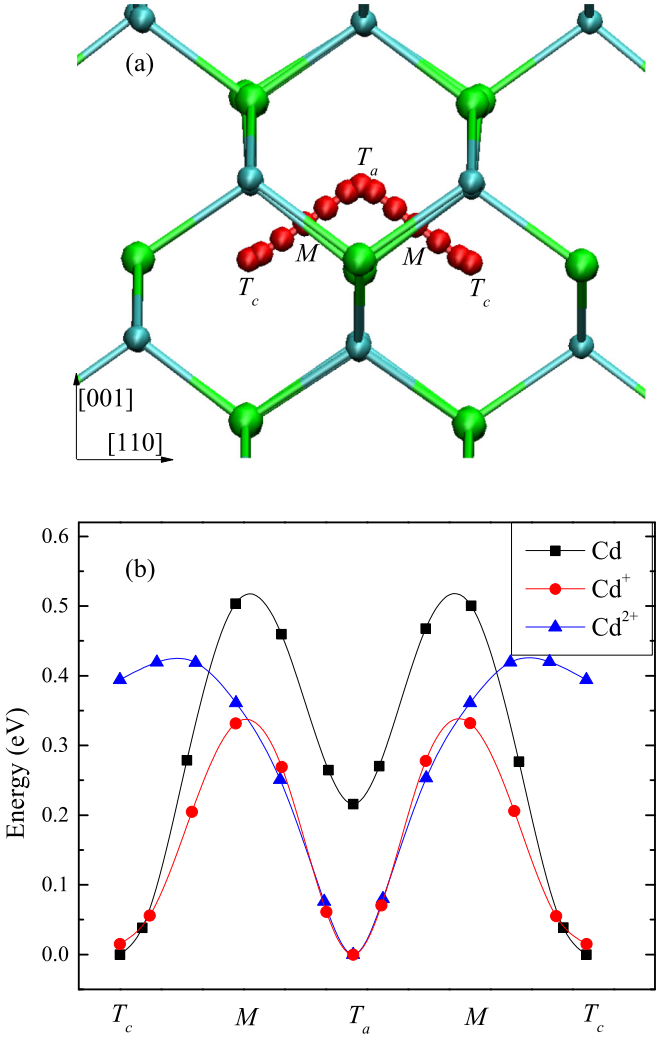

FIG. 1. (Color online) The diffusion path (a) and diffusion energy curves (b) of the interstitial Cd atom. In (a), the cyan balls represent Cd, the green balls represent Te, and the diffusion path of the interstitial Cd atom is highlighted in red. The diffusion paths are the same for neutral and charged Cd atoms. The energy of the most stable site is set to zero in (b). The black squares (Cd), red dots (Cd^+), and blue triangles (Cd^{2+}) represent the energies of the NEB images, and the lines are spline fittings.

energy. For Cd^+, the diffusion barrier site is still the M site, but the energy barrier decreases to ∼0.34 eV. This is because the size of Cd^+ is smaller than that of neutral Cd, so the strain energy at the M site is smaller for Cd^+. For Cd^{2+}, the Coulomb interaction is strong and also plays a role. It largely increases the energy at the T_c site; on the other hand, because the size of Cd^{2+} is even smaller, the strain energy at the M site is significantly reduced. Therefore Cd^{2+} at the M site has a lower energy than the T_c site, and the diffusion barrier site appears in between the M and T_c sites, with an energy barrier of ∼0.42 eV. Because of the interplay between the Coulomb effect and the strain effect, the diffusion barrier energy first decreases and then increases, as Cd changes from neutral to 1+ to 2+ charged states.

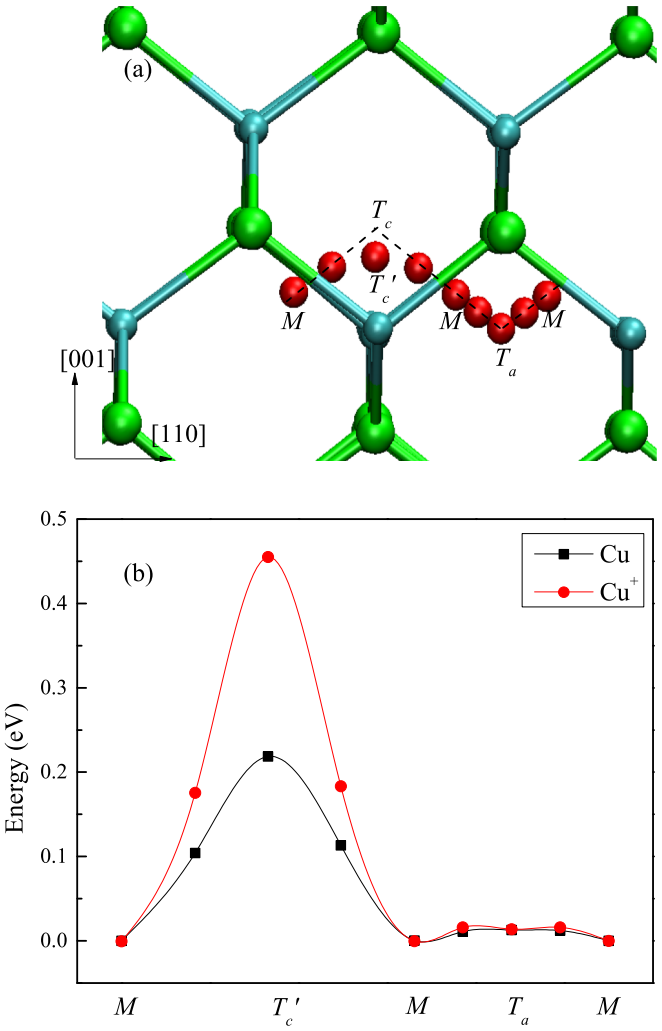

FIG. 2. (Color online) The diffusion path (a) and diffusion energy curves (b) of the interstitial Cu atom. In (a), the cyan balls represent Cd, the green balls represent Te, and the diffusion path of the interstitial Cu atom is highlighted in red. The dashed lines indicate the [111] and [11$\bar{1}$] directions. The diffusion paths are similar for neutral and charged Cu atoms. The energy of the most stable site is set to zero in (b). The black squares (Cu) and red dots (Cu^+) represent the energies of the NEB images, and the lines are spline fittings.

2. Cu *diffusion*

Cu is a fast diffuser in many semiconductors. The fast diffusion behavior has been explained by the *s-d* coupling between Cu *d* orbitals and host *s* orbitals [21]. The interstitial Cu is a shallow single donor in CdTe, and thus it can exist in two charge states: neutral and 1+ charged state.

The diffusion path of the interstitial Cu is displayed in Fig. 2(a). The diffusion paths of the neutral and 1+ charged Cu atoms are similar. Different from the Cd diffusion, Cu does not diffuse along the exact ⟨111⟩ directions and does not cross the exact tetrahedral sites. This abnormal diffusion behavior has been explained by the strong *s-d* coupling [21]. In the Cd diffusion case, because the *d* electron of Cd is much lower in energy, the *s-d* coupling is rather weak, and thus the diffusion still follows exactly the ⟨111⟩ directions. In the Cu diffusion case, because the Cu 3*d* orbital is higher in energy and more delocalized, the *s-d* coupling is much stronger, especially at the *M* site which has low symmetry [21]. We find that for both Cu and Cu^+, the *M* and T_a sites are almost degenerate in energy. Therefore the diffusion energy curves are almost flat around the T_a site. Because the *M* site, which is the diffusion barrier site in the Cd diffusion case, is pulled down in energy, the diffusion barrier site appears at the T_c' site for both neutral and charged Cu. Because the positively charged Cu^+ gain more *s-d* coupling energy at the *M* site and has larger Coulomb repulsions near the T_c' site that is surrounded by positively charged host Cd ions, the diffusion energy barrier of Cu^+ (∼0.46 eV) is higher than that of neutral Cu by ∼0.25 eV.

B. Anion diffusions

In this section, we will discuss the diffusions of two anion atoms, namely, Te and Cl. Because the defect electrons occupy the degenerated *p*-like states, there always exist large structural distortions, depending on the electron occupations on the defect levels. Therefore the diffusions are not along the ⟨111⟩ directions, and strongly depend on the charge states of the interstitial anion atoms.

1. Te *diffusion*

The neutral interstitial Te at T_c or T_a site is an deep acceptor with two holes on triplet-degenerated t_2 states [14]. However, as we discuss above, this configuration is unstable because the system can gain electronic energy through the level-splitting induced by the structural distortion. According to our calculations, the most stable interstitial site of the neutral Te is the split-interstitial (Spl) site [20,22], which is displayed in Fig. 3(a). At this site, the interstitial Te atom (Te_2) shares a lattice site with the original host Te atom (Te_1). When the interstitial Te is at the Spl site, the triplet-degenerated states are splitted into three nondegenerated states (Fig. 4). The first two states, which are fully occupied, decrease in energy, and the third one, which is fully empty, increases in energy, compared to the degenerated t_2 states, so the level-splitting lowers the electronic energy. However, at the tetrahedral sites, there is more space around the interstitial Te, so the strain energy is relatively low; but at the Spl site, the strain energy increases. The competition between the electronic energy gain and strain energy cost determines the most stable site. Our calculations show that because the system can gain a large amount of the electronic energy for the neutral Te, the Spl site becomes the most stable one. It is very interesting to see that after the structural distortion, the nominally acceptor of Te interstitial becomes a deep double donor. Moreover, we find that it is a negative U system, i.e., it has only two stable charge states, namely, neutral and 2+ charged states [20].

First, we consider the diffusion of the neutral interstitial Te. The diffusion of the neutral interstitial Te is displayed in Fig. 3. At first [Fig. 3 (a)], the interstitial Te (Te_2) shares a lattice site with the host Te (Te_1), and then it diffuses along the [110] direction to a nearby lattice site [Fig. 3(c)] sharing with another host Te (Te_3). The diffusion barrier appears when Te_2 is nearly in the middle between the Te_1 and Te_3 sites [Fig. 3(b)], with an energy barrier of ∼0.1 eV. In the following step, the original interstitial Te_2 will kick out Te_3 and occupy the host site by itself. The original host Te_3 now becomes the new

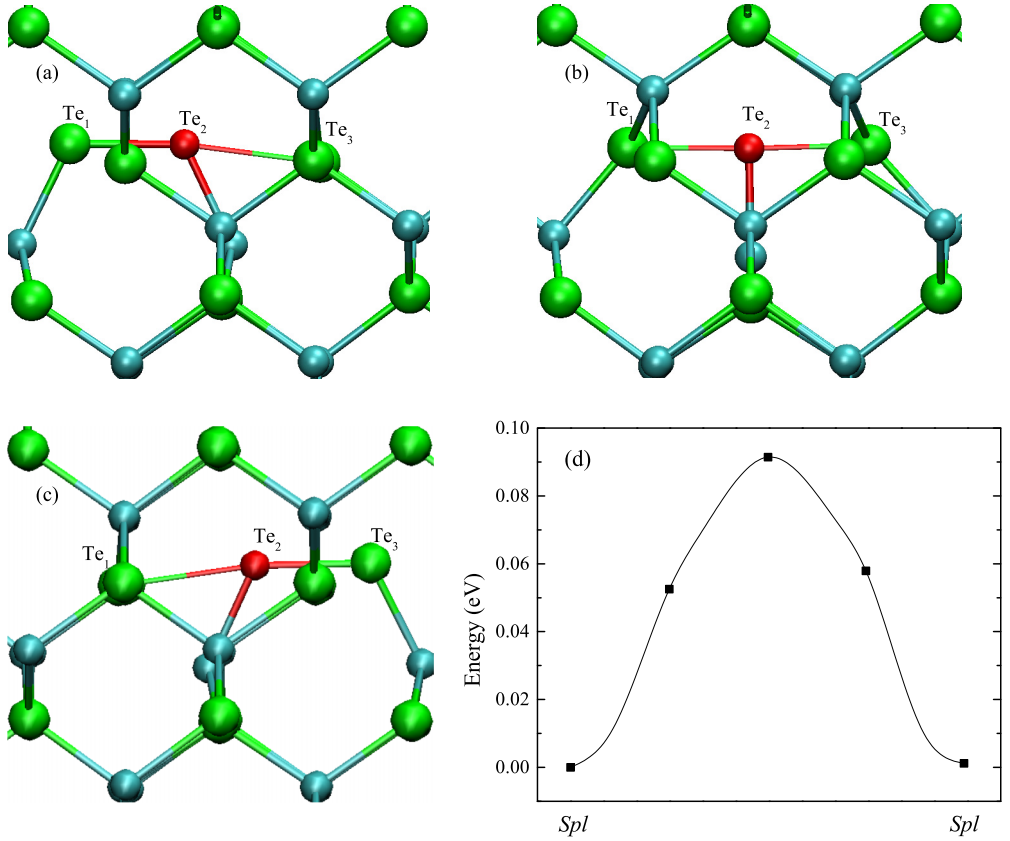

FIG. 3. (Color online) The most stable site (a) and (c), diffusion barrier site (b), and diffusion energy curve (d) of the neutral interstitial Te. In (a)–(c), the cyan balls represent Cd, the green balls represent Te, and the interstitial Te is highlighted in red. The energy of the most stable site is set to zero in (d). The black squares represent the energies of the NEB images, and the line is a spline fitting.

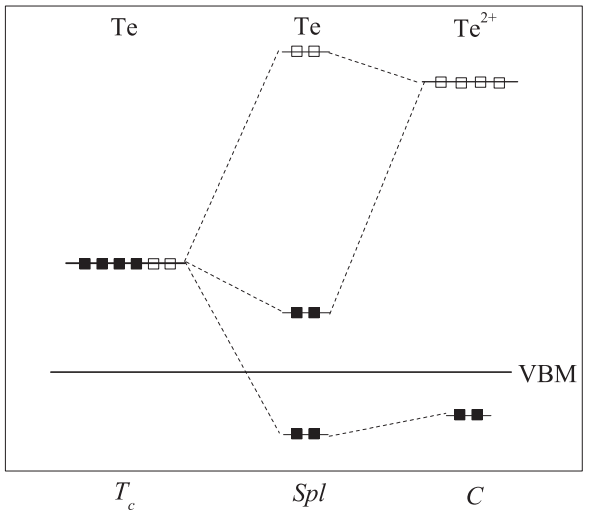

FIG. 4. The schematic energy positions of defect levels of Te at the T_c, Spl, and C sites. The filled squares represent electrons and open ones represent holes. At the T_c site, the symmetry is T_d and the defect levels are the triplet-degenerated t_2 states, which are occupied by four electrons (two holes). At the Spl site, the symmetry is broken so that the t_2 states are splitted into three nondegenerated states. For neutral Te, the first two states are fully occupied and the last one is empty. At the C site, the t_2 states are splitted into a fully occupied nondegenerated state below the VBM and doublet-degenerated states. For Te^{2+}, the doublet-degenerated states are fully empty.

interstitial Te and keeps diffusing along the ⟨110⟩ directions. By this diffuse-and-kick-out process, Te can diffuse very fast along the ⟨110⟩ directions.

Next, we consider the 2+ charged state. In this state, two electrons are removed from the defect levels, so the electronic energy gain becomes less at the Spl site (Fig. 4), and therefore, the Spl site is no longer the most stable site. Instead, the most stable interstitial site of Te^{2+} is the C site, which is displayed in Fig. 5(a). At this site, the interstitial Te (Te_1) is almost in the center among three host Te atoms. When Te^{2+} is at this site, the local symmetry is C_{3v}, and the defect levels are splitted into a nondegenerated state below the VBM and doublet-degenerated states above the t_2 state. Because the singlet state is fully occupied and the doublet-degenerated states are fully empty, the system gains the most electronic energy in this structure. At the C site, there is more space around the interstitial Te than that at the Spl site, so the strain energy at the C site is relatively low. Therefore it becomes the most stable site for Te^{2+}.

The diffusion of the 2+ charged interstitial Te^{2+} is displayed in Fig. 5. At first [Fig. 5(a)], Te_1 is at the interstitial C site. In the diffusion process, Te_1 kicks out the original host Te_2 from the lattice site. Finally, Te_1 occupies the lattice site, and Te_2 becomes the new interstitial Te and starts to diffuse along the ⟨110⟩ directions [Fig. 5(c)]. The diffusion barrier appears when Te_1 and Te_2 share the lattice site. This diffusion barrier is actually the Spl site [Fig. 5(b)], which is the most

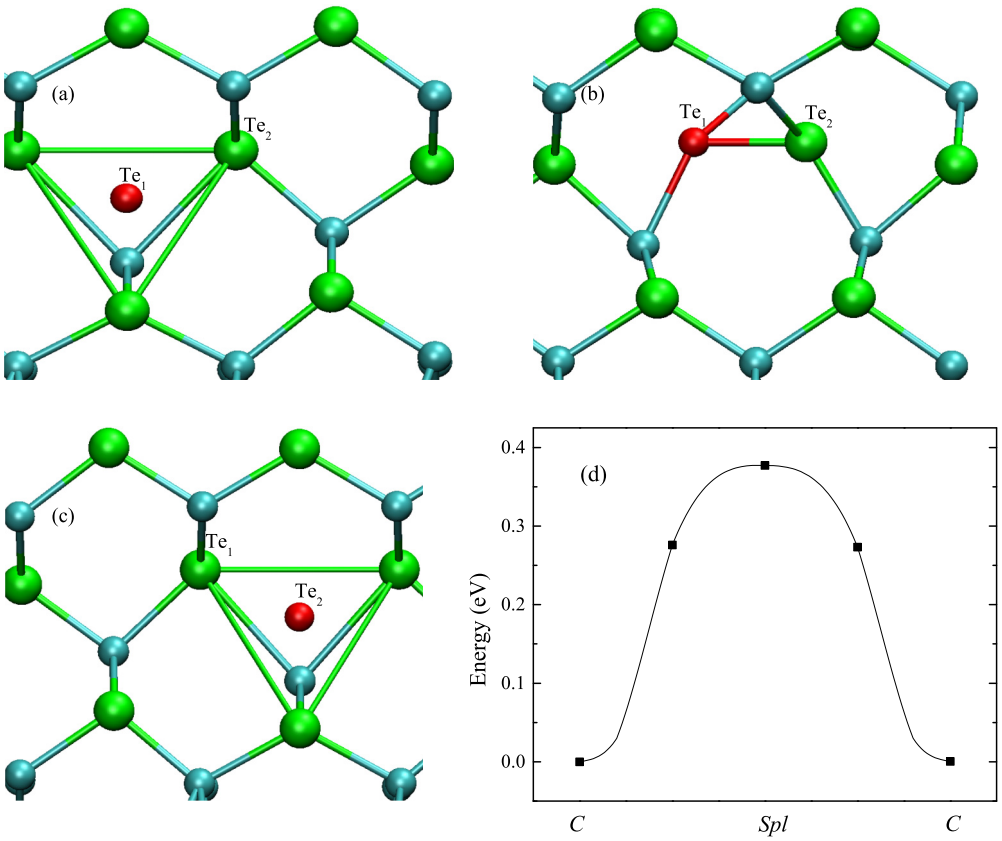

FIG. 5. (Color online) The most stable site (a) and (c), diffusion barrier site (b), and diffusion energy curve (d) of the 2+ charged interstitial Te^{2+}. In (a)–(c), the cyan balls represent Cd, the green balls represent Te, and the interstitial Te is highlighted in red. In (a), Te_1 is the interstitial atom. In (b), Te_1 and Te_2 share the same lattice site (Spl structure). In (c) Te_1 enters the lattice site and kicks out Te_2, which becomes the new interstitial atom. The energy of the most stable site is set to zero in (d). The black squares represent the energies of the NEB images, and the line is a spline fitting.

stable site for the neutral Te, and the diffusion barrier energy is ∼0.4 eV. Apparently, the 2+ charged Te^{2+} diffuses much slower than the neutral Te.

2. Cl *diffusion*

The interstitial Cl is a shallow single acceptor in CdTe. The relative positions of the defect levels of an interstitial Cl at different sites are displayed in Fig. 6. When the interstitial Cl is at the T_c site, the triplet-degenerated defect levels are even below the VBM in energy. In this case, an electron on the VBM will drop to the defect level and a hole is created on the VBM. Therefore the defect levels are fully occupied and the interstitial Cl already accepts an electron becoming the Cl^- state. The T_c site is actually the most stable site for interstitial Cl. At the T_c site, the defect transition energy level is even below the VBM [23], so the interstitial Cl can only be at the 1− charged state. However, in the diffusion, as the local symmetry is reduced, the degenerated levels split and the highest level could be above the VBM in energy. Therefore, in the diffusion process, the interstitial Cl can be either at neutral state or 1− charged state. In the diffusion of interstitial Cl, there exists a neutral to 1− charge transition. Because the defect level of Cl only has one hole, the crystal-field splitting generally cannot release enough energy to stabilize distorted structures. However, in the case of Cl in CdTe, the exchange splitting is large due to the relatively localized Cl $3p$ state. When the interstitial Cl stays in the middle between two nearest-neighboring Cd atoms, which is labeled as the B_c site here (see Fig. 8), the energy is only 2 meV higher than that at the T_c site. The local density of states (LDOS) of Cl p state at B_c site is presented in Fig. 7. We can see clearly the large exchange splitting (around 0.5 eV), which can stabilize the structure. Therefore, Cl can generate a steady magnetic moment in CdTe. It is well known that $2p$ and $3d$ electrons can generate a steady magnetic moment [24], but here the steady magnetic moment is generated by Cl $3p$ electrons. However, at the T_c sites, because the defect levels are fully occupied, there is no magnetic moment.

The diffusion of the interstitial Cl is displayed in Fig. 8. Cl first diffuses from the T_c site to the B_c site. As Cl moves away from the tetrahedral site, the degenerated defect states split. At first, the splitting is small, and hence, all the splitted states are below the VBM in energy. In this case, Cl is still at 1− charged state. Because all the defect states are fully occupied, the system cannot gain any electronic energy. However, the strain energy keeps increasing, so the system energy increases. When the splitting increases so that the highest splitted state is higher in energy than the VBM, Cl is transferred into the neutral state. In this case, because there is a hole on the defect level, the exchange splitting lowers the total energy of the system. Therefore the diffusion barrier appears when

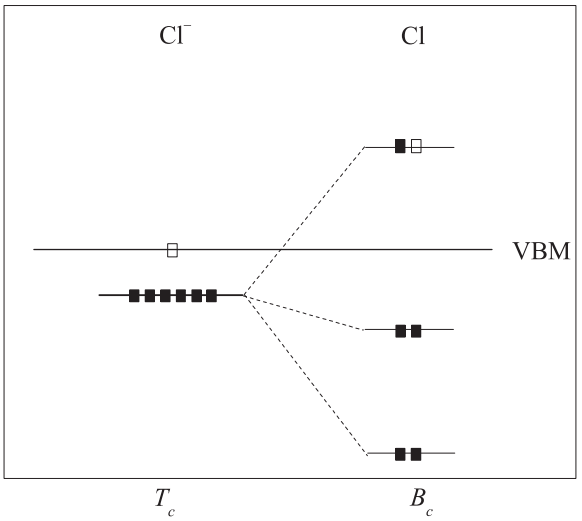

FIG. 6. The schematic energy positions of defect levels of Cl at the T_c site and B_c site. The filled squares represent electrons and open ones represent holes. At the T_c site, the symmetry is T_d and the defect levels are the triplet-degenerated t_2 states. Because the defect levels of Cl are below the VBM, Cl already accepts an electron from the VBM and becomes Cl^-. At the B_c site, the symmetry is broken so that the t_2 states are splitted into three nondegenerated states. Two of them are still below VBM and the last one is inside the band gap. In this case, Cl becomes neutral. In this figure, the exchange splitting is not included.

the highest defect level is close to the VBM in energy. The diffusion barrier energy is ∼0.1 eV. After arriving at the B_c site, Cl then diffuses to another nearby B_c site. In this step, Cl is always at the neutral state and there is a hole on the defect level. Because the electronic energy gained from the exchange splitting almost offsets the strain energy, the diffusion energy curve is quite flat in this step and the diffusion energy barrier is only 25 meV. In the final step, Cl diffuses from the B_c site to a new T_c site and finishes the whole diffusion process. In

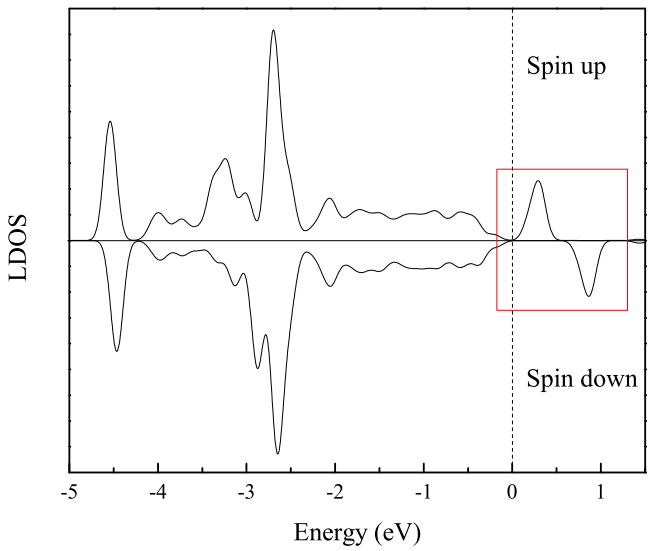

FIG. 7. (Color online) The LDOS of Cl p states at the B_c site. The dashed line indicates the VBM of the host. We can clearly observe the exchange splitting (∼0.5 eV) above the VBM in the red rectangle.

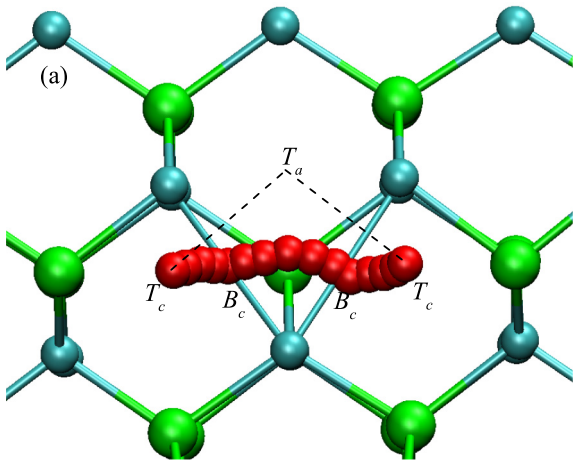

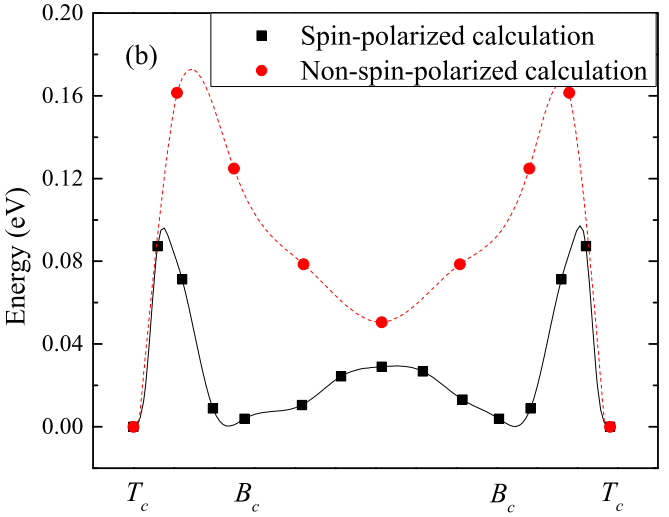

FIG. 8. (Color online) The diffusion path and diffusion energy curve of Cl. It first diffuses from the T_c site to a B_c site, then diffuses from the B_c to a nearby B_c site, and finally diffuses from the new B_c site to a new T_c site. In (a), the cyan balls represent Cd, and green balls represent Te, and the diffusion path of the interstitial Cl is highlighted in red. The dashed lines indicate [111] and [11$\bar{1}$] directions. The energy of the T_c site is set to zero in (b). The black squares represent the energies of the NEB images, and the line is a spline fitting. The red dots are calculated without spin polarization. Apparently, the exchange splitting plays an important role in decreasing the diffusion energy barrier.

the diffusion, Cl overcomes three barriers: a small one with the energy of 25 meV and two equivalent barriers with the energy of 0.1 eV. In Fig. 8, we also plot the diffusion energy curve of Cl calculated without spin polarization. Apparently, without spin polarization, the energies of the low-symmetry sites are higher than those calculated with spin polarization, which indicates the exchange splitting plays an important role in decreasing the diffusion energy barrier.

Next, we consider the 1− charged state. When calculating Cl^-, we put an extra electron into the system. Therefore, no matter at which site, Cl is always at 1− charged state and all the defect levels are always fully occupied. In this case, the distorted structure cannot gain energy from any level splittings. Therefore the diffusion of Cl^- is from T_c (the most stable

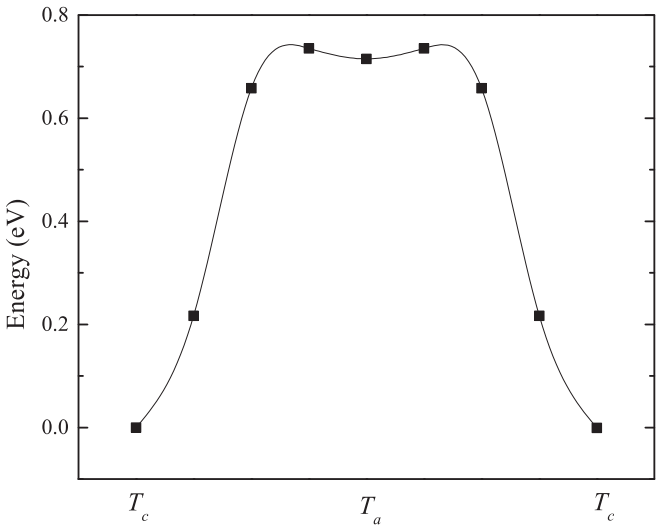

FIG. 9. The diffusion energy curve of Cl^-. The energy of the T_c site is set to zero. The black squares represent the energies of the NEB images, and the line is a spline fitting. The diffusion path of Cl^- is similar to that of Cd.

site) to T_a (transition site) and then to another T_c, which is exactly the same as the cation diffusions. The diffusion barrier energy is increased to ∼0.7 eV (Fig. 9). Again, the charged Cl^- diffuses much slower than the neutral Cl.

IV. CONCLUSIONS

In summary, using first-principles DFT calculations, we have studied the diffusions of interstitial cation atoms (Cd and Cu) and anion atoms (Te and Cl) in CdTe. We have established the connection between the diffusion behavior and the electronic structure of the interstitial diffuser. For the cation atoms, because the defect electrons occupy the nondegenerated s-like state under the T_d symmetry, the diffusions are almost along the ⟨111⟩ directions between the tetrahedral sites, although the diffusion of Cu shows some deviation due to the s-d coupling. The diffusions of the neutral and charged cation atoms follow similar paths. However, for the anion atoms, because the defect electrons occupy the p-like triplet-degenerated states under the T_d symmetry, there always exist large structural distortions. Therefore the diffusions follow totally different paths, and strongly depend on the charge states of the interstitial diffusers. The physical reason for the distortions are different: for Te, the distortion is stabilized by the crystal-field splitting, but for Cl, the exchange splitting plays a more important role.

ACKNOWLEDGMENTS

The work at National Renewable Energy Laboratory was funded by the U.S. Department of Energy under Contract No. DE-AC36-08GO28308. Some of the calculations were carried out using the National Energy Research Scientific Computing Center supercomputers supported by US DOE under Contract No. DE-AC02-05CH11231.

[1] J. Nissilä, K. Saarinen, P. Hantojärvi, A. Suchocki, and J. M. Langer, Phys. Rev. Lett. **82**, 3276 (1999).
[2] R. Biswas and Y. P. Li, Phys. Rev. Lett. **82**, 2512 (1999).
[3] S. B. Zhang, S.-H. Wei, and A. Zunger, J. Appl. Phys. **83**, 3192 (1998).
[4] G. M. Dalpian and S.-H. Wei, Phys. Rev. B **72**, 075208 (2005).
[5] S. Guha, J. M. DePuydt, M. A. Hasse, J. Qiu, and H. Cheng, Appl. Phys. Lett. **63**, 3107 (1993).
[6] W. Shockley and H. J. Queisser, J. Appl. Phys. **32**, 510 (1961).
[7] C. H. Henry, J. Appl. Phys. **51**, 4494 (1980).
[8] Best Research-Cell Efficiencies, available at http://www.nrel.gov/ncpv/images/efficiency_chart.jpg.
[9] D. H. Rose, F. S. Hasoon, R. G. Dhere, D. S. Albin, R. M. Ribelin, X. S. Li, Y. Mahathongdy, T. A. Gessert, and P. Sheldon, Prog. Photovolt: Res. Appl. **7**, 331 (1999).
[10] T. A. Gessert, W. K. Metzger, P. Dippo, S. E. Asher, R. G. Dhere, and M. R. Young, Thin Solid Films **517**, 2370 (2009).
[11] L. Zhang, J. L. F. Da Silva, J. Li, Y. Yan, T. A. Gessert, and S.-H. Wei, Phys. Rev. Lett. **101**, 155501 (2008).
[12] J. Ma, S.-H. Wei, T. A. Gessert, and K. K. Chin, Phys. Rev. B **83**, 245207 (2011).
[13] H. Jahn and E. Teller, Proc. R. Soc. London, Ser. A **161**, 220 (1937).
[14] S.-H. Wei and S. B. Zhang, Phys. Rev. B **66**, 155211 (2002).
[15] W. Kohn and L. J. Sham, Phys. Rev. **140**, A1133 (1965).
[16] J. P. Perdew, K. Burke, and M. Ernzerhof, Phys. Rev. Lett. **77**, 3865 (1996).
[17] G. Kresse and J. Furthmuller, Phys. Rev. B **54**, 11169 (1996).
[18] G. Kresse and D. Joubert, Phys. Rev. B **59**, 1758 (1999).
[19] G. Mills and H. Jonsson, Phys. Rev. Lett. **72**, 1124 (1994).
[20] J. Ma, D. Kuciauskas, D. Albin, R. Bhattacharya, M. Reese, T. Barnes, J. V. Li, T. Gessert, and S.-H. Wei, Phys. Rev. Lett. **111**, 067402 (2013).
[21] J. Ma and S.-H. Wei, Phys. Rev. Lett. **110**, 235901 (2013).
[22] M.-H. Du, H. Takenaka, and D. J. Singh, J. Appl. Phys. **104**, 093521 (2008).
[23] K. Biswas and M.-H. Du, New J. Phys. **14**, 063020 (2012).
[24] H. Peng, H. J. Xiang, S.-H. Wei, S.-S. Li, J.-B. Xia, and J. Li, Phys. Rev. Lett. **102**, 017201 (2009).